PROCESSING OF DIELECTRIC MATERIALS AND METALS WITH PS LASERPULSES

Paper (M101)

Beat Neuenschwander[1], Guido F. Bucher[1], Guido Hennig[2], Christian Nussbaum[1], Benjamin Joss[1], Martin Muralt[1], S. Zehnder[1], Urs W. Hunziker[1] and Peter Schütz[1]

[1] Bern University of Applied Sciences, Engineering and Information Technology
Pestalozzistrasse 20, Burgdorf, 3400, Switzerland
[2]Dätwyler Graphics, Flugplatz, Bleienbach, 3368, Switzerland

Abstract

Ever since industrially applicable ps laser systems have been available, cold ablation with ultra short laser pulses is of huge interest when high requirements concerning accuracy, defined surface roughness and small heat affected zone are demanded. Interesting applications are in the fields of surface and 3-d structuring with direct and induced processes. For a profitable industrial use of this technology high process efficiency is required, which is enabled by the development of systems with high average power of more than 100 W. The process efficiency directly scales with the average power when the repetition rate of the system is properly chosen. But aside from process efficiency often a high surface quality (low surface roughness, minimized surface melting and no oxidation processes) is desired. These measures are not only strongly affected by the laser parameters but also by the strategy of structuring. Especially for surface structuring the corresponding requirements for the equipment of the beam guiding system are often not accomplishable and therefore there is a strong demand for new technologies which have to be developed.

Introduction

The development of industrial applicable ultra short pulsed laser systems toward pulse energies from a few µJ up to a about 100 µJ at repetition rates from some 10 kHz up to a few MHz has strongly increased the interest in using these pulses for micro material processing in the industrial field. Compared to ns-pulses from Q-switched systems, ultra short pulses show less thermal effects due to the significantly reduced thermal penetration depth. Furthermore, in the case of isolators, one can benefit from nonlinear effects as for example multi-photon absorption or tunneling ionization which are nearly absent for ns-pulses.

For metals the energy and heat-transfer process is described with the two temperature model [1], where the temperatures of the free electrons, absorbing the energy of the laser pulse, and the lattice are treated separately. The time for the energy transfer from the free electrons to the lattice, the electron-phonon thermalization time, amounts a few ps [2,3]. A further reduction of the pulse duration will not lead to additional benefits in terms of the threshold fluence [2,3,4], rather it can lead to a reduced precision and to increased unwanted plasma effects [3,4]. As high power ps-systems are mostly set up as master oscillator post amplifier (MOPA) systems without pulse stretcher and compressor they can be built very stable and more efficient compared to fs-systems. For high precision laser micro processing of metals, systems with pulse durations of a few ps are therefore the method of choice with respect to economical considerations.

In contrast to metals, the high band gap in dielectric materials leads to a completely different situation. As reported in [5] the threshold fluence drops with the pulse duration also in the low fs regime. This fact can be explained with the probability for nonlinear effects as multi-photon absorption, tunneling ionization or frequency conversion, which significantly increases with decreasing pulse duration. However, also for these materials nice results can be achieved with ps-pulses.

Beside all these advantages one has also to obtain a high throughput to be competitive to other laser systems or alternative technologies. This was one of the motivations to develop ps laser systems with average powers up to more than 50W which are today available e.g. from Time-Bandwidth Products, Lumera or Trumpf. But to really take benefit of these high average powers, one has to optimize the whole chain from the laser parameters over the beam guiding system to the process and the process strategies. A very interesting industrial application is the removal of thin films e.g. the removal of thin amorphous semiconductor films for thin film solar cells. This is often called the P1-, the P2- and P3-scribe [6]. Laser

systems with ps pulses are well suited for all three scribes, but depending on the used material for the cells, sometimes with different wavelengths for the single scribes.

In the following this article will concentrate on another interesting application often used in printing industries [7], the generation of small 3-dimensional structures especially on metal surfaces.

Generation of 3d structures

In most applications the generation of 3d-structures is realized in a 2½d-process where the structure is divided into several slices as shown in Fig. 1a.

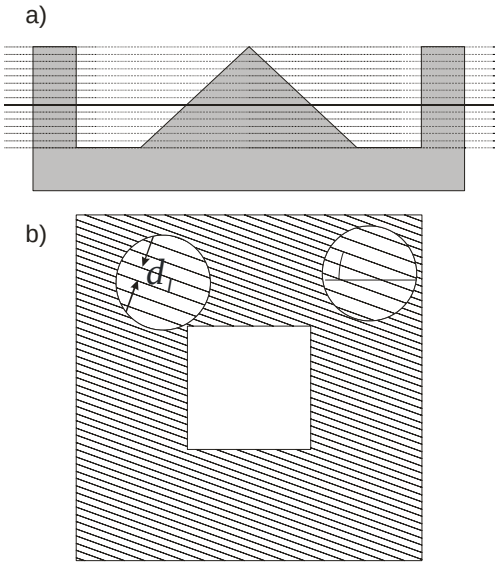

Fig. 1: Generation of 3d structures with a 2½d-process.

The outline of each slice which has to be removed is filled with parallel or rectangular crossed lines as shown in Fig. 1b. The parallel lines are seperated by the distance d_l and are rotated by the angle α with respect to the horizontal. The minimum line distance d_l is limited on the one hand by the scanner resolution and on the other hand by the used scanner software. For the experiments presented here a Raylase Superscan with a 10 mm aperture was used for the both wavelengths 352nm and 355nm. Here the minimum line distance d_l is limited to 7 µm for a f = 100 mm f-Θ-objective @532 nm and to 9 µm for a f = 110mm telezentric objective @ 355 nm. A DUETTO ps-laser system from Time-Bandwidth products was used for the structuring experiments. This system generates pulses of about 10 ps pulse duration at repetition rates from 50 kHz to 1 MHz with a beam quality $M^2 < 1.3$. A second special amplifier box contains an electro optic modulator which works from 50kH to 300kHz repetition rate. Whit this pulse picker the repetition rate can be further reduced down to single shot and the beam can be switched on and off. The fundamental wavelength amounts 1064 nm and can be doubled and tripled to 532 nm and 355 nm.

Fig. 2 shows three different structures generated in sapphire with 355 nm wavelength. The lateral dimension of the stamp on the left and the skewed pyramid are in the vertical range of 1 mm whereas the structure on the right side has a lateral dimension of 1.5 mm. These examples clearly show that transparent materials can be well machined with ps laserpulses.

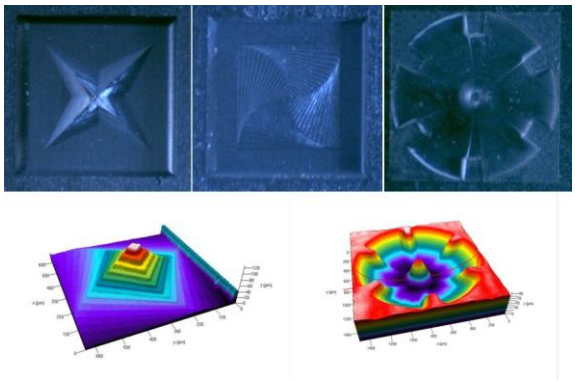

Fig. 2: 3d-structures machined into sapphire with corresponding topographies.

Fig. 3 shows on the left side the topography of Switzerland and on the right side a special structure machined with 532 nm wavelength in copper. The lateral dimensions here amount 9.8 mm for the topography of Switzerland and 2.5 mm for the structure.

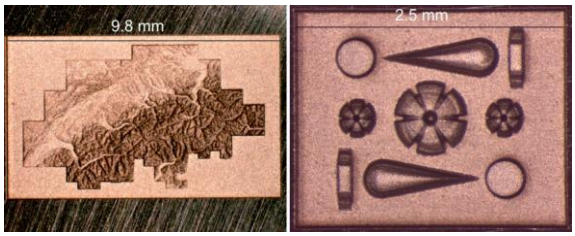

Fig. 3: 3d-structures machined into copper.

The presented examples show that the presented 2½-d strategy is well suited for the generation of 3d structures in metals and dielectric materials.

Process optimization

Surface quality

The surface quality, i.e. surface roughness and homogeneity, strongly depends on the process strategy. Fig. 4 shows the bottom of a structure when the outline of each slice is filled with parallel rectangular crossed lines. The structure at the bottom directly corresponds to the line pattern and deep grooves are observed.

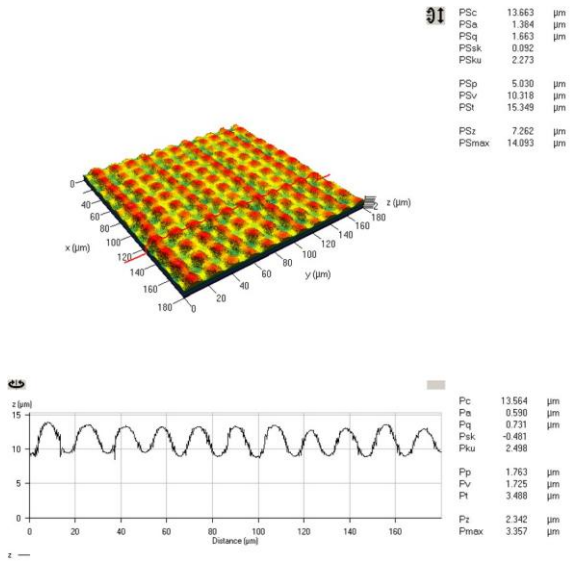

Fig. 4: Surface pattern on the bottom of a structure when each slice is filled with parallel and rectangular crossed lines. At the bottom a line cut, corresponding to the red line in the top, is shown,

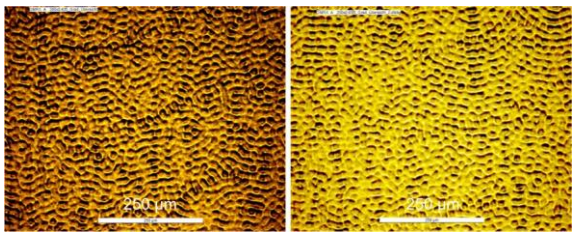

Fig. 5: Surface pattern on the bottom of a structure when the angle of the rectangular crossed lines is changed from slice to slice in steps of 5° in ascending order (left side) and arbitrary order (right side).

This drawback can be reduced by varying the angle α (see Fig.1) from slice to slice. On the left side of Fig. 5 the pattern at the bottom of the structure for parallel rectangular crossed lines is shown, when the angle α is turned in steps of 5° from 0° to 90°. The surface structure is less pronounced but shows still some kind of periodicity. The turn angles (0°, 5°, 10°, ..., 90°) can also be arranged in arbitrary order. The corresponding result is shown in Fig. 5 on the right side. Both strategies actually lead to the same result. Similar behaviour has been observed for other turn angle steps.

In contrast, the situation changes when the distance d_l between the lines is reduced. The used scanner has a resolution of 16 bit and a scan field of 110mmx110mm for a 100 mm f-theta objective. This leads to a theoretical minimum line distance of about 1.7 µm. The minimum distance which can be set in the used scanner software WeldMark1.0 is four times bigger than the limit given by the resolution. Enlarging the spot radius would help to improve the surface homogeneity but is at the expense of precision and this is mostly unwanted.

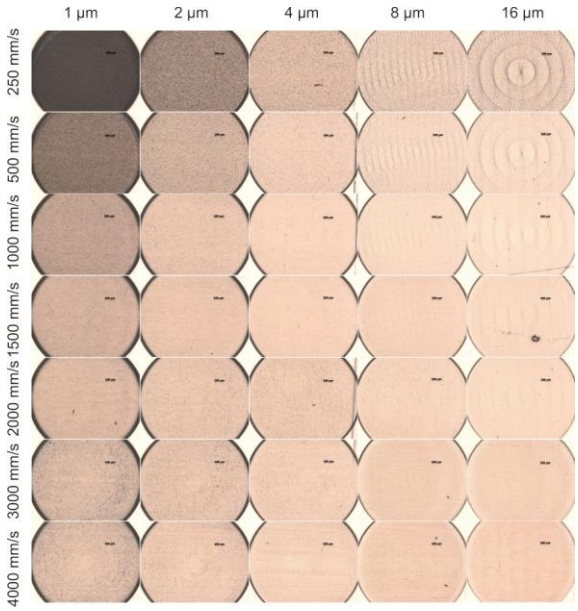

Fig. 6: Overview of the parameter study for copper at the average power of 250 mW.

The problem with the limited line distance can be avoided when the filling lines of the outline are all drawn in a graphic program and imported into the scanner software in a vector graphic format. With this, in principle line distances down to the theoretical limit of the scanner can be realized. For a parameter study circles of 1.5 mm diameter were filled with parallel lines and, from slice to slice, the angle α was turned in steps of 5° from -90° to 90° which results in 37 slices. The parameter study was performed for polished copper at a laser wavelength of 532 nm with a spot radius of 7 µm and a repetition rate of 250 kHz and for sapphire and borosilicate glass with 355 nm wavelength with a spot radius of 5 µm and a repetition rate of 200 kHz. The study for copper was done for average powers of 125 mW, 250 mW and 500 mW,

whereas 750 mW was the average power for borosilicate glass and sapphire.

Fig. 6 shows the result for copper and an average power of 250 mW. The line distance is increased by a factor of two from column to column and the marking speed is increased for each row from top down. The corresponding values are denoted in the figure. Note that the line distance of 1 µm is below the physical resolution of the scanner and therefore can't be marked correctly. A pronounced surface pattern within the circles was observed for line distances of 8 µm and 16 µm also for high marking speeds. A quite homogeneous surface is obtained for a line distance of 4 µm and markings speeds of 1000 mm/s or more.

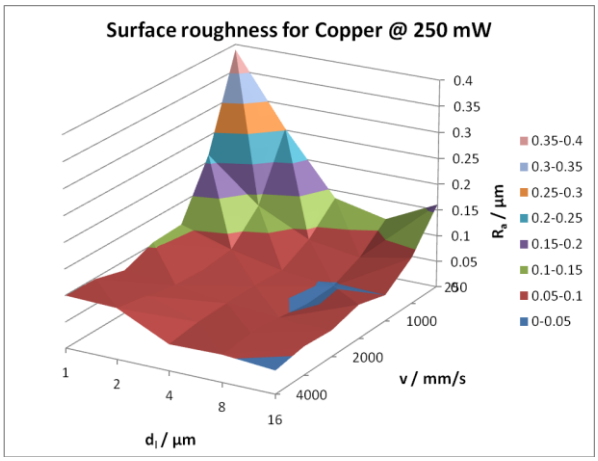

Fig. 7: R_a values for the parameter study with copper for an average power of 250 mW.

The corresponding surface roughness in terms of the R_a values is shown in Fig. 7. For most of the parameters a surface roughness of less than 100 nm is obtained. It can clearly be seen that small line spacing and low marking speed lead the highest surface roughness of more than 0.3 µm. In general, the surface roughness decreases when line distance increases from 1 µm to 4 µm. This may be caused by heat accumulation for small line distances. As one is at the physical resolution limit with these small line distances this may also be caused by imprecise marking due to noise. On the opposite side a line distance of 8 µm or 16 µm, which leads to a pronounced surface pattern as shown in Fig. 6, does not automatically correspond to a high roughness. Also with theses distances a surface roughness less than 100 nm was achieved at marking speeds higher than 500 mm/s. But for a homogeneous surface the ideal line spacing is in the range of 4 µm and the lowest surface roughness of about 60 nm is obtained for marking speeds between 1000 mm/s and 3000 mm/s. With a spot radius of 7 µm and the repetition rate of 250 kHz these speeds correspond to a spacing of about one spot radius from pulse to pulse. Also for the average powers of 125 mW or 500 mW the most homogeneous surface with the best roughness are obtained for a line distance of 4 µm and marking speeds between 1000 mm/s and 3000 mm/s. The corresponding R_a-values amount about 40 nm for 125 mW and 130 nm for 500 mW average power. This shows that the R_a values increases with the average power.

The results for copper can be summarized as follows: To obtain a homogeneous surface with low roughness the line distance should be about half the spot radius and the spacing between two pulses has to be in the range of one spot radius. The surface roughness clearly increases with the average power and therefore with the pulse energy.

The situation, especially for low marking speeds and large line distances, dramatically change for sapphire as can be seen in Fig. 8. Here the highest roughness of about 3 µm is achieved for a line distance of 16 µm and a marking speed of 200 mm/s. Note that the marking speeds for sapphire are downscaled relative to copper due to the smaller repetition rate of 200 kHz. Also for sapphire homogeneous surfaces with low roughness are obtained under the same conditions as for copper i.e. a line distance in the range of half a spot radius and a pulse to pulse spacing of about one spot radius. In contrast to copper the surface roughness is much higher and amounts to about 300 nm which is roughly one magnitude higher. For borosilicate it is again higher and amounts about 400 nm.

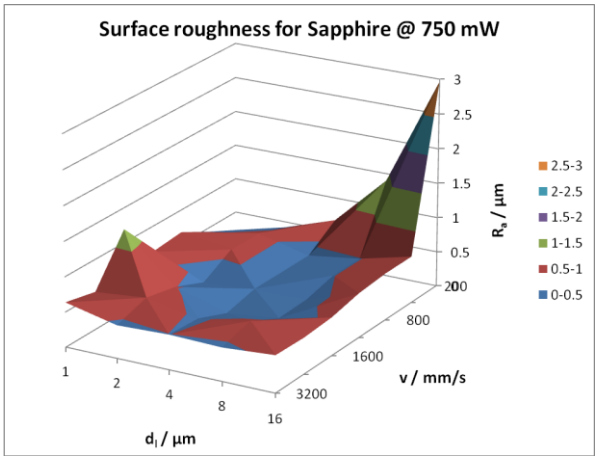

Fig. 8: R_a values for the parameter study with sapphire for an average power of 750 mW.

Structuring strategy

Fig. 2 and 3 and the left side of Fig. 9 show that the presented method is well suited to generate surface structures with lateral dimensions in the mm range. But when the dimension of the structures is reduced to less than about 100 µm, the scanner resolution limits the obtainable accuracy as shown in the right of Fig. 9.

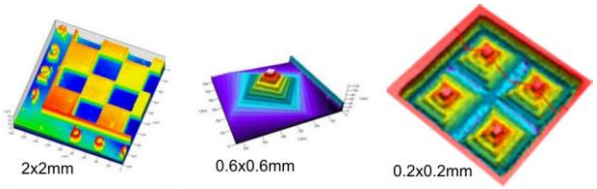

Fig. 9: 3d-structures with dimensions in the range mm (left side) and in the range of 100 µm (right side).

With an adapted strategy structures with these dimensions can be machined. Figure 10 shows a 100µm side length positive and negative shaped pyramid copper.

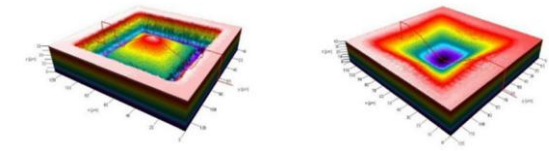

Fig. 10: Negative (right) and positive (left) shaped pyramid with 100µm side length in copper.

The pyramids in figure 10 were machined with two crossed linear stages. The stages stopped always at the desired position and one pulse was fired onto the target, and the pyramids were also built up slice by slice. With this of course slow method, many different structuring strategies can be easily tested. A strategy which allows the machining of such small structures with small surface roughness is illustrated in figure 11. One slice consists of several layers. In one layer single pulses are concatenated in the distance of about one spot diameter (this spacing corresponds to the demands presented in the previous paragraph). From layer to layer the pattern is shifted in a defined sequence. With such strategies a surface roughness of less than 50 nm can be achieved also in the walls of the structure.

To apply the above strategy the spot diameter should not become larger than 1/10 of the lateral structure dimension. To shift the pattern from layer to layer in a defined way, the resolution of the beam guiding system has to be about ¼ of the spot radius. For a structure with 100 µm lateral dimension this corresponds to a spot radius of maximum 5 µm and to a resolution of about 1 µm. For a 100mm x 100mm working field and assuming 2 bits of noise this leads to a minimum resolution of 19 bit for the beam guiding system.

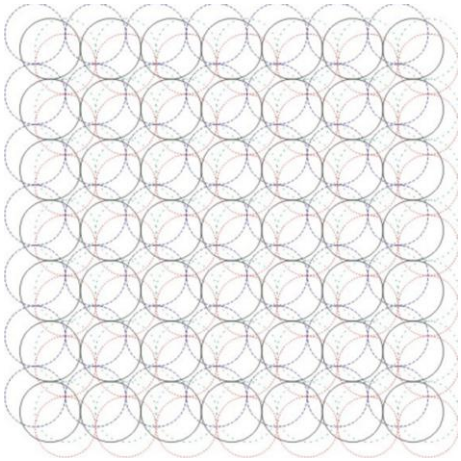

Fig. 11: A possible strategy to generate small pyramids. Each slice is divided into several layers. In one layer the pulses are concatenated in the distance of the spot radius.

Due to assimilated heat it will not be possible to generate such a single structure with 100 µm lateral dimension with an average power in the range of a few Watts as offered from today ps laser systems. To prevent from overheating the average power has to be distributed over an adequate surface area i.e. multiple structures have to be generated in one work item. This can only be realized with fast linear stages or with galvo scanners at high resolution.

As high power ps systems (and also fs systems) are mostly set up as master oscillator post amplifier (MOPA) systems the beat of the laser pulses is finally given by the seed laser of the system. As long as the beam guiding system is synchronized with the pulse train of the laser system the uncertainty of the starting pulse for a single line amounts about one spot diameter. When e.g. a rectangle is set up from different parallel lines, this uncertainty leads to an inaccuracy of the structure as shown in the left of fig. 12. To overcome this drawback the seed laser signal should be used as a clock pulse for the electronic control of the beam guiding system. Whit this, the situation shown on the right in fig. 12 could be realized and the accuracy of the machined structure could significantly increased.

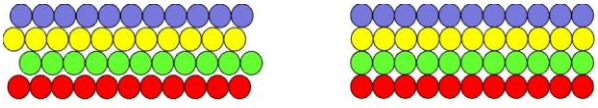

Fig. 12: Rectangle marked with four lines without (left) and with (right) synchronization of the beam guiding system and the laser pulse train.

Ablation rate

It is a consequence of the two temperature model for pulses [1] and often reported in the literature e.g. [8,9], that for short and ultra short pulses the ablation depth z_{abl} logarithmically depends on the laser pulse fluence ϕ:

$$z_{abl} = \delta \cdot \ln\left(\frac{\phi}{\phi_{th}}\right) \qquad (1)$$

Where δ is some kind of penetration depth of the energy and ϕ_{th} denotes the threshold fluence for which the ablation process starts. One can now ask for the difference between one pulse with energy E_P and fluence ϕ_p or n pulses with energy E_P/n and fluence ϕ_p/n. Under the assumption that in the case of multiple pulses the result of each pulse is not influenced by the leading pulse, the ablation depth is given by:

$$z_{abl}(n) = n \cdot \delta \cdot \ln\left(\frac{\phi_{tot}}{n \cdot \phi_{th}}\right) \qquad (2)$$

Fig. 13 shows the ablation curve corresponding to (1) for ϕ_{th} = 1 J/cm^2 and δ = 500 nm as blue line. The result of the ablation depth for a total fluence (n = 1) of 10 J/cm^2 corresponding to (2) is shown with red dots. It is obvious that a clear maximum ablation depth exist for n = 4.

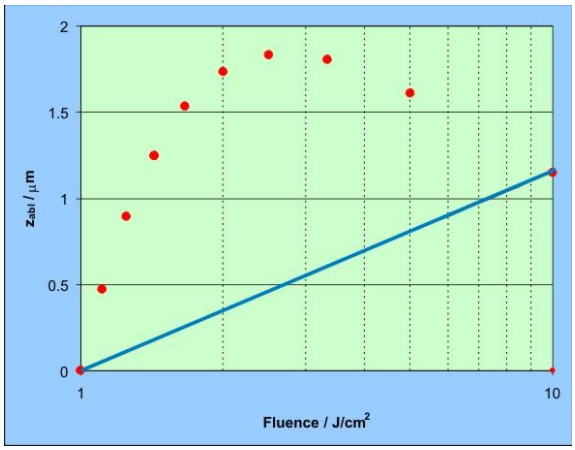

Fig. 13: Ablation curve (blue) for ϕ_{th} = 1J/cm^2 and δ = 500nm and the total ablation depth corresponding to (2) for a total fluence of 10 J/cm^2.

A short calculation leads to:

$$n_{opt} = \frac{1}{e} \cdot \frac{\phi_{tot}}{\phi_{th}}\ ;\ z_{abl,\max} = \frac{\delta}{e} \cdot \frac{\phi_{tot}}{\phi_{th}} \qquad (3)$$

Note that the optimum pulse number n_{opt} does not automatically correspond to a nonnegative integer in this calculation. For a pulse with a Gaussian shaped intensity distribution of radius w_0 the local fluence is a function of the distance r to the beam centre:

$$\phi(r) = \phi_0 \cdot e^{-2 \cdot \frac{r^2}{w_0^2}} \qquad (4)$$

with

$$\phi_0 = \frac{2 \cdot E_p}{\pi \cdot w_0^2} \qquad (5)$$

When (4) is inserted in (1) the ablated volume of a pulse of a Gaussian shaped beam can be calculated according to [10], it amounts to

$$\Delta V = \frac{1}{4} \cdot \pi \cdot w_0^2 \cdot \delta \cdot \ln^2\left(\frac{\phi_0}{\phi_{th}}\right) \qquad (6)$$

For a laser system with a constant average power P working at the repetition rate f the pulse energy is given by $E_p = P/f$ and the total ablated volume per time amounts to

$$\dot{V} = f \cdot \Delta V \qquad (7)$$

Inserting (5) and (6) into (7) lead to:

$$\dot{V} = \frac{1}{4} \cdot \pi \cdot w_0^2 \cdot \delta \cdot f \cdot \ln^2\left(\frac{2 \cdot P}{f \cdot \pi \cdot w_0^2 \cdot \phi_{th}}\right) \qquad (8)$$

For a given average power P, threshold fluence ϕ_{th}, penetration depth δ and spot size w_0 the ablation rate $\dot{V}$ depends on the repetition rate.

The blue dots in Fig. 14 show the measured volume ablation rate on a polished copper surface with a constant average power of 3 W, a wavelength of 1064 nm and a spot radius of 19.5 µm. The repetition rate was varied in 25 kHz steps from 25 kHz up to 300 kHz. The red line in fig. 14 is the least square fit of the model function (8) to the measured data. The resulting threshold fluence amounts to 1.07 J/cm^2 and the penetration depth is 33 nm.

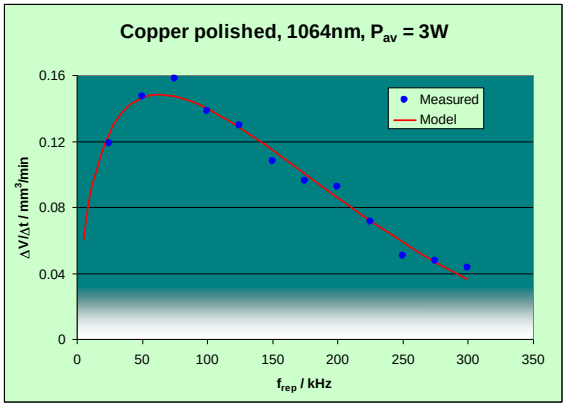

Fig. 14: Model (red line) and measured data of the volume ablation rate for copper.

The measured values agree very good with the model function according to (8). This is also confirmed for steel 1.4301 as shown in fig. 15. Here the threshold fluence (ϕ_{th} = 0.08 J/cm^2) and the penetration depth (δ = 5.5 nm) were deduced from an ablation experiment and introduced into the model function (8). Also here a very good agreement between the model function and the measured volume ablation rate is observed.

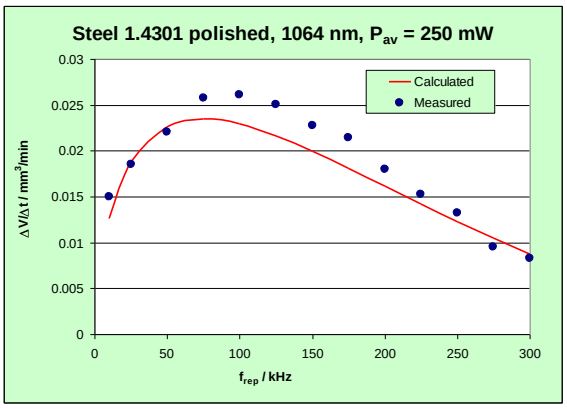

Fig. 15: Model (red line) and measured data of the volume ablation rate for steel 1.4301.

The experimentally confirmed model function clearly shows a maximum ablation rate $\dot{V}_{\max}$ at an optimum repetition rate f_{opt} for a given average power. The corresponding values can be derived from (8) and amount:

$$f_{opt} = \frac{1}{e^2} \cdot \frac{2 \cdot P}{\pi \cdot w_0^2 \cdot \phi_{th}} \qquad (9a)$$

$$\dot{V}_{\max} = 2 \cdot \frac{\delta}{e^2} \cdot \frac{P}{\phi_{th}} \qquad (9b)$$

Both, the optimum repetition rate and the maximum ablation rate linearly scales with the average power, i.e. doubling of the average power leads to a doubled ablation rate the at the optimum repetition rate.

In [11,12] it is reported that with ps-pulse bursts the ablation rate can be increased by a factor of up to 10. Having a look to the typical form of the model function with a strong gradient at low repetition rates a part of this increase could also be explained by the fact that the energy of one pulse is divided into several pulses with the pulse bursts. This can also be treated as a simple increase of the repetition rate.

Summary

For precise and efficient machining with ps laser pulses of structures with lateral dimension ℓ with optimum surface homogeneity and roughness one has to consider the following points:

- The spot diameter $2w_0$ should not exceed 1/10 of the lateral structure dimension, i.e. $w_0 \le \ell / 20$.
- The resolution Δx of the beam guiding system should be at least ¼ of the spot radius, i.e. $\Delta x \le w_0 / 4$.
- The optimum spacing between two pulses should be bigger than one spot radius w_0. The corresponding marking speed v then depends on the repetition rate f and amounts: $v \ge f \cdot w_0$
- When the outline of a slice is filled with parallel lines, the optimum distance d_l between this lines is given by $d_l \approx w_0 / 2$.
- The beam guiding system should be synchronized with the beat of the laser pulses for structure dimension of less than 100 µm.
- For a given fixed average power there exist an optimum repetition rate (9a) where a maximum volume ablation rate (9b) going with the highest process efficiency can be achieved.

Applying these points to a structure of 100 µm lateral dimension into steel 1.4301 (ϕ_{th} = 0.08 J/cm^2 and δ = 5.5 nm) this leads to the following numbers:

The spot radius should amount at least 5 µm and the resolution has to be about 1.25 µm corresponding to a

18 – 19 bit range for a 100mm x 100mm working field. The beam guiding system has to be synchronized with the beat of the laser pulses. To work at the optimum point with maximum ablation rate the optimum repetition rate in terms of the average power P_{av} reads:

$$f_{opt} \approx 4.3 \frac{MHz}{W} \cdot P_{av}$$

The corresponding maximum ablation rate is the given by:

$$\dot{V}_{\max} \approx 0.11 \frac{mm^3}{min} \cdot \frac{1}{W} \cdot P_{av}$$

The marking speed in terms of the average power then reads:

$$v \approx 20 \frac{m}{s} \cdot \frac{1}{W} \cdot P_{av}$$

In this case a marking speed of 100 mm/s is therefore desired for an average power of 5 W. With a conventional galvo scanner a maximum marking speed of about 5 m/s can be obtained at the desired spot radius of 5 µm, i.e. the point of maximum ablation rate can only be obtained up to an average power of about 400 mW. For higher average powers the optimum spacing between two pulses can still be guaranteed with the fixed repetition rate of 1 MHz but the pulse energy has to be increased i.e. one can' t work at the optimum point. Following (8) the ablation rate is then still increasing but only weak following a squared logarithm of the average power instead linearly.

Conclusions

Laser pulses in the low ps range ($\Delta\tau \approx 10ps$) are very well suited for laser micro processing of metals and also dielectric materials. With adapted strategies it is possible to machine 3d-structures with very high accuracy and a surface roughness below 100 nm into surfaces. But one is not able to work at the optimum point for the today offered average powers. There is therefore a great lack of beam guiding systems to really take benefit of state of the art ps laser systems. The beam guiding systems have to be fastened to marking speeds in the range of 100 m/s to work with average powers in the rage of 10 W. Further the systems have to be synchronized with the beat of the laser pulse train to reach the optimum accuracy.

References

[1] B.N. Chichkov, C. Momma, S. Nolte, F. van Alvensleben and A. Tünnermann (2001), Femtosecond, picosecond and nanosecond laser ablation of solids, Applied Physics A, 63, 109-115

[2] G. Mourou et al. (2002), Method for controlling Configuration of laser induced breakdown and ablation, US Patent US RE37,585 E

[3] Friedrich Dausinger, Helmut Hügel and Vitali Konov (2003), Micro-machining with ultrashort laser pulses: From basic understanding to technical applications, Proc. SPIE, 5147, 106-115

[4] Detlef Breitling, Andreas Ruf and Friedrich Dausinger (2004), Fundamental aspects in machining of metals with short and ulrashort laser pulses, Proc. SPIE 5339, 49-63

[5] M. Lenzer, J. Krüger, S. Sartania, Z. Cheng, Ch. Spielmann, G. Mourou, W. Kautek and F. Kausz (1998), Femtosecond Optical Breakdown in Dielectrics, Physical Review Letters 80, 4076-1079

[6] S. Lauzurica, et al (2009), Comparitive study on nanosecond and picoseconds laser patterning of thin film for photovoltaic solar moduls based on a-Si:H, in Proceedings of the fifth international WLT conference on lasers in manufacturing, 635 – 640

[7] G. Hennig, K-H. Selbmann, J. Brendel, S. Brüning, P. Dietiker and B. Neuenschwander (2009), Laserstrukturierung grossflächiger Tiefdruckwalzen mit Mikropräzision, in Tagungsband Laser in der Elektronikproduktion & Feinwerktechnik

[8] M. Hashida et al (2002), Ablation threshold dependence on pulse duration for copper, Applied surface science, 197-198, pp. 862-867

[9] P. Mannion, J. Magee, E. Coyne and G.M. O'Conner (2003), Ablation thresholds in ultrafast laser micro-machining of common metals in air, in Proceedings SPIE 4876, 470 – 478

[10] B. Neuenschwander et al (2010), Processing of metals and dielectric materials with ps-laserpulses: results, strategies, limitations and needs, in Proc. SPIE, 7584-26

[11] C. Hartmann and A. Gillner (2007), Investigation on laser micro ablation of steel using ps-IR pulse bursts, in LIA Conference Proceedings, LIA, Orlando, 38–44

[12] Ralf Knappe et al (2010), Scaling ablation rates for picosecond lasers using burst micromachining, in Proc. SPIE, 7585-16

Meet the Author

Beat Neuenschwander studied physics at the University of Bern and realized 1996 his PhD at the institute of applied physics. Since 2000 he is at the Bern University of Applied Sciences where he built up the laboratory for laser micro machining. He lectures physics and applied laser technology and is currently managing director of the SwissLaserNet SLN and head of the optics section of the Swiss Society for Optics and Microscopy SSOM.